

## Not so non-marine? Revisiting the Stoer Group and the Mesoproterozoic biosphere

E.E. Stüeken<sup>1,2,3\*</sup>, E.J. Bellefroid<sup>4</sup>, A. Prave<sup>1</sup>,  
D. Asael<sup>4</sup>, N.J. Planavsky<sup>4</sup>, T.W. Lyons<sup>2</sup>



### Abstract

doi: 10.7185/geochemlet.1725

The Poll a'Mhuilt Member of the Stoer Group (Torridonian Supergroup) in Scotland has been heralded as a rare window into the ecology of Mesoproterozoic terrestrial environments. Its unusually high molybdenum concentrations and large sulphur isotope fractionations have been used as evidence to suggest that lakes 1.2 billion years ago were better oxygenated and enriched in key nutrients relative to contemporaneous oceans, making them ideal habitats for the evolution of eukaryotes. Here we show with new Sr and Mo isotope data, supported by sedimentological evidence, that the depositional setting of this unit was likely connected to the ocean and that the elevated Mo and S contents can be explained by evapo-concentration of seawater. Thus, it remains unresolved if Mesoproterozoic lakes were important habitats for early eukaryotic life.

Received 10 November 2016 | Accepted 15 May 2017 | Published 13 June 2017

### Introduction

Important steps in early biotic evolution may have occurred in lakes that offered distinct environmental conditions compared to the ocean. Support for this hypothesis has been reported from the Mesoproterozoic Poll a'Mhuilt Member (Stoer Group) in Scotland, which is interpreted as a fluvio-lacustrine deposit (Stewart, 2002). Parnell *et al.* (2010; 2015) documented large S isotope fractionations (up to 55 ‰) and Mo concentrations reaching 232 ppm that far exceed those of most contemporaneous marine shales. These features were interpreted as

an indication that Mesoproterozoic lacustrine environments were more oxygenated and nutrient-rich than seawater, making them preferable habitats for eukaryotic organisms. However, the supposition that the Poll a'Mhuilt Member was deposited in a lacustrine setting rests on contestable lines of evidence: fluvial sandstones bracketing the proposed lacustrine interval and allegedly high boron concentrations in illite, which were regarded as ambiguous in the original study (Stewart and Parker, 1979; Stewart, 2002). Here we present new geochemical data and sedimentological features that indicate a marine influence, particularly during deposition of the Mo- and S-rich interval.

### Geologic Setting

The mostly siliciclastic Stoer Group rests nonconformably on Archaean gneiss in northwest Scotland (Stewart, 1988). The depositional age is constrained to  $1177 \pm 5$  Ma based on  $^{40}\text{Ar}$ – $^{39}\text{Ar}$  dating on diagenetic K-feldspar in the Stac Fada Member, an ancient impact deposit (Parnell *et al.*, 2011; Reddy *et al.*, 2015) immediately beneath the Poll a'Mhuilt Member (Fig. 1).

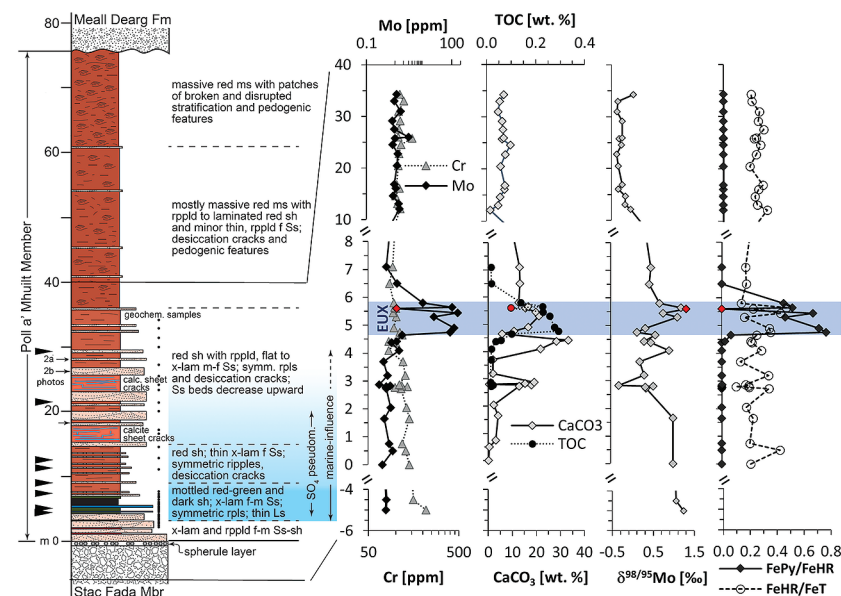


**Figure 1** Stratigraphy of the Poll a'Mhuilt Member. EUX = euxinic interval. The 5.6 m (red symbols) was affected by modern oxidative weathering and is not considered in the discussion. Black arrows = locations of tidal indicators.

1. School of Earth and Environmental Sciences, University of St. Andrews, St. Andrews, Fife, KY16 9AL, Scotland, UK
2. Department of Earth Sciences, University of California, Riverside CA 92521, USA
3. Virtual Planetary Laboratory, University of Washington, Seattle WA 98195, USA
- \* corresponding author (email: ees4@st-andrews.ac.uk)
4. Department of Geology and Geophysics, Yale University, New Haven CT 06520, USA



The basal ~3 m of the Poll a' Mhuil Member consist of channelled, trough cross-bedded and planar laminated sandstone overlain by about 1–2 m of mottled grey-red shale with thin limestone beds followed up section by 2–4 m of calcareous dark grey shale. The limestone beds contain small-scale, chicken-wire fabric (calcite and albite pseudomorphs replacing gypsum). The carbonate is mostly micro-crystalline (Fig. S-1); secondary calcite replacements are minor. The next ~25 m consist of red shale and thin sandstone with abundant desiccation cracks and flat-laminated to ripple cross-laminated, 5–50 cm-thick beds of fine to medium sandstone which have abundant symmetrical (wave) ripples and locally developed herringbone cross-lamination (Fig. 2b), as well as flaser and lenticular bedding (Fig. 2a) and evaporite pseudomorphs after gypsum (Parnell *et al.*, 2010). The overlying (and major) part of the Poll a' Mhuil Member (>~30 m) comprises massive red mudstone and flat-laminated to ripple cross-laminated fine sandstone and siltstone, all with desiccation cracks and pedogenic structures, such as disrupted and homogenised beds and pseudo-anticlines (Stewart, 2002).



**Figure 2** Sedimentary features compatible with a marine setting in the middle Poll a' Mhuil Member. (a) Flaser- and lenticular-bedding. (b) Superposed sets of herringbone cross-lamination, 3D exposures confirm bi-directional character. Stratigraphic positions are marked in Figure 1. (c) Line drawing of sedimentary features showing superposed sets of bi-polar cross-laminated ripples (herringbone) with multiple reactivation surfaces commonly with thin clay drapes.

## Methods

We collected outcrop samples extending from the upper 5 m of the Stac Fada Member through 35 m of the Poll a' Mhuil Member, with emphasis on the calcareous grey shale (4.75 to 5.80 m, Fig. 1) (58.202422°N, 5.340425°W). Our analytical methods follow standard protocols as described in the Supplementary Information, with the exception of our carbonate-Sr extraction. As silicate phases can release Sr during acid-dissolution, we extracted carbonate-bound Sr with a ten-step sequential leaching procedure (modified after Liu *et al.*, 2013). This approach allowed us to construct a mixing curve between carbonate and silicate phases, where the latter can be monitored with Rb. The pure carbonate end-member was calculated by extrapolation to a Rb/Sr ratio of zero. Bedrock samples were analysed for Sr isotopes after bulk digestions and back-calculated to 1.2 Ga using measured Rb/Sr ratios and the  $^{87}\text{Sr} \leftarrow ^{87}\text{Rb}$  decay constant to account for  $^{87}\text{Rb}$  decay.

## Results

Similar to Parnell *et al.* (2015), we found high Mo concentrations of up to 166 ppm in the grey shale of the Poll a' Mhuil Member (4.75–5.80 m), which is 180 times higher than in the surrounding red shales (Fig. 1). Other transition metals show weak to no enrichments in the grey shale (Table S-3). Nickel and Cr are elevated in the volcanic/impact breccia of the Stac Fada Member and then decrease slowly into the Poll a' Mhuil Member.

Ratios of highly reactive Fe ( $\text{Fe}_{\text{HR}}$ ; bound in oxides, sulphides and carbonates) to total Fe ( $\text{Fe}_{\text{T}}$ ) fall between 0.15 and 0.49 in the grey shale unit, while ratios of pyrite-bound Fe ( $\text{Fe}_{\text{Py}}$ ) to  $\text{Fe}_{\text{HR}}$  range from 0.46 to 0.78 (Fig. 3a). Carbon to sulphur ratios range from 0.1 to 1.2 (median 0.2) in the grey shale. Molybdenum isotope data show positive values in the Stac Fada Member (+1.15 ‰), then progressively decrease in the first red shale (~0 m to 4 m), followed up section by an increase to a maximum of +1.19 ‰ in the grey shale (5.65 m, Fig. 1). In the overlying red shale (12 to 33 m),  $\delta^{98}\text{Mo}$  drops to -0.38 ‰. Carbonate  $\delta^{18}\text{O}$  and  $\delta^{13}\text{C}$  values throughout the section covary (Fig. 3b). Carbonate-bound  $^{87}\text{Sr}/^{86}\text{Sr}$  ratios in the red and grey shale (4.10–5.65 m) trend toward end-members of 0.707–0.710 (Fig. 3c). Two gneiss samples from the Lewisian basement, back-calculated to 1.2 Ga, have  $^{87}\text{Sr}/^{86}\text{Sr}$  ratios of  $0.721 \pm 0.008$ ; two amphibolite dyke samples and two Stac Fada samples average around  $0.704 \pm 0.002$  and  $0.706 \pm 0.0004$ , respectively.

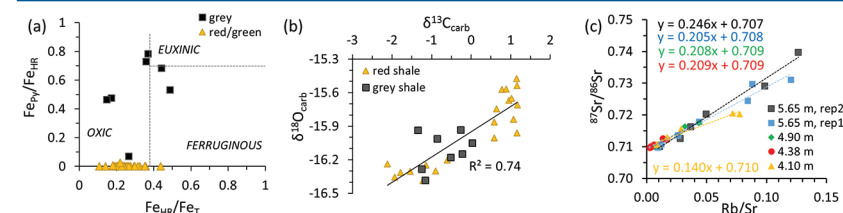


**Figure 3** (a) Iron speciation, (b) carbonate C and O isotopes, and (c) carbonate-bound Sr isotopes. Dashed lines in (a) mark redox transitions (Poulton and Canfield, 2011). For comparison to our data in panel (b), values of contemporaneous unaltered marine carbonates fall between -10 ‰ and -7 ‰ for  $\delta^{18}\text{O}_{\text{carb}}$  and 0 ‰ and +2 ‰ for  $\delta^{13}\text{C}_{\text{carb}}$  (Shields and Veizer, 2002) (see Fig. S-2 for discussion). In panel (c), data points represent individual leaches increasing acid strength; y-axis intercept = carbonate end-member.

## Discussion

Some sedimentary features in the Poll a' Mhuil Member provide unequivocal evidence for a largely subaerial depositional setting: the basal (<3 m) channelised and trough cross-bedded sandstones and unimodal palaeocurrent indicators imply fluvial deposition (Stewart, 2002) and the abundant pedogenic features



in the upper part (30 m) of the member indicate deeply palaeo-weathered alluvium (Stewart, 2002). However, within the 3–30 m interval that contains the calcareous and grey shale we observed flaser, pin-stripe and lenticular bedding; multiple reactivation surfaces; mud drapes and herringbone cross-lamination (Fig. 1). These features are strong evidence of tidally influenced sedimentation on marine tidal flats (Davis Jr., 2012). Closely interfingered marine and non-marine deposition is not uncommon in the rock record. For example, recent discoveries of tidal indicators in the Ordovician Juniata Formation raised doubts about some of the oldest purported evidence for land colonisation by animal life (Davies *et al.*, 2010). Our sedimentological observations raise similar concerns for the eukaryotic biota of the Stoer Group (Cloud and Germs, 1971). This view is supported by our geochemical data, which are most parsimoniously explained by a marine influence during the deposition of the middle Poll a'Mhuilt Member (~3–30 m).

Carbonate-bound  $^{87}\text{Sr}/^{86}\text{Sr}$  ratios capture the isotope composition of the water column in which the carbonate precipitated. As typical continental runoff is more radiogenic ( $^{87}\text{Sr}$ -enriched) than seawater,  $^{87}\text{Sr}/^{86}\text{Sr}$  values can distinguish between marine and non-marine environments (Veizer *et al.*, 1990; Spencer and Patchett, 1997). However, infiltration of secondary fluids during early or late diagenesis typically increases carbonate  $^{87}\text{Sr}/^{86}\text{Sr}$  ratios (Banner and Hanson, 1990). Covariation and low values of  $\delta^{18}\text{O}_{\text{carb}}$  and  $\delta^{13}\text{C}_{\text{carb}}$ , as seen in our samples, may indicate some degree of alteration by continental fluids (Fig. 3c) (Shields and Veizer, 2002; Bartley and Kah, 2004). However, alteration almost always leads to more radiogenic carbonate  $^{87}\text{Sr}/^{86}\text{Sr}$  ratios (Banner and Hanson, 1990). Diagenetic fluids were likely sourced from the surrounding land surface and should have reflected the composition of the Lewisian tonalite-trondjemite-granodiorite gneiss ( $0.740 \pm 0.033$ ; Lyon *et al.*, 1975; this study; and see Supplementary Information for discussion). Therefore, the  $^{87}\text{Sr}/^{86}\text{Sr}$  ratio of our least radiogenic carbonate end-member (0.707, Fig. 3b), directly from within the sulphide- and Mo-rich interval (Parnell *et al.*, 2015), provides a maximum constraint for the primary  $^{87}\text{Sr}/^{86}\text{Sr}$  ratio of the water body from which the carbonate precipitated. This value is too low to reflect exclusively continental runoff from the Lewisian basement ( $>0.715$ ), which should dominate the signal in a lacustrine setting. Instead, this value is better explained by mixing between fluvial and marine waters. The latter have an estimated composition of 0.705–0.706 at 1.2 Ga (Kuznetsov *et al.*, 2014).

Repetitive influxes of seawater, followed by evaporation, would favour the precipitation of gypsum as recorded by pseudomorphs in the middle Poll a'Mhuilt Member (3–30 m, Fig. 1). As previously proposed (Parnell *et al.*, 2010, 2015), a combination of proxies—including large S isotope fractionations consistent with pyrite formation in the water column, high Mo/Re ratios and large amounts of pyrite despite low TOC contents (low C/S ratios)—suggest that the water column turned euxinic (sulphidic) during the evaporitic phase, perhaps as a result of salinity stratification and cut-off from seawater inflow. This pattern is supported by the Fe chemistry (see Supplementary Information for detailed discussion). Briefly, in the grey shale,  $\text{Fe}_{\text{HR}}/\text{Fe}_{\text{T}}$  ratios at the upper end of the detrital threshold (Raiswell and Canfield, 1998, also inferred from red shales in

our study) are consistent with some iron enrichment under anoxic conditions, and  $\text{Fe}_{\text{Py}}/\text{Fe}_{\text{HR}}$  ratios of up to 0.8 are consistent with euxinia (Poulton and Canfield, 2011). This interpretation is bolstered by the observed high Mo levels that are almost always associated with at least intermittent euxinia in the modern and ancient ocean (Scott and Lyons, 2012). The red shales lack  $\text{Fe}_{\text{HR}}/\text{Fe}_{\text{T}}$  enrichments (Fig. 3a), consistent with oxic deposition at water depths probably shallower than those for the grey shale (Stewart, 2002).

Although seawater probably had low Mo levels at this time (*e.g.*, 1–10 nM, Reinhard *et al.*, 2013), the presence of gypsum pseudomorphs implies that the water in this setting evaporated by a factor of up to 11 (assuming 100 % Mesoproterozoic seawater with modern levels of dissolved  $\text{Ca}^{2+}$  and  $\leq 2$ –10 mM  $\text{SO}_4^{2-}$ ; Kah *et al.*, 2004; Luo *et al.*, 2014), which could have locally raised dissolved Mo concentrations (perhaps to near-modern levels of 105 nM). Ensuing euxinia would have pulled this concentrated Mo reservoir into sediments. Repeated seawater incursions, evapo-concentration and euxinia could have acted like a Mo pump, sustaining these sedimentary Mo enrichments.

The Mo isotope data are consistent with a marine influence. The  $\delta^{98}\text{Mo}$  of seawater can be effectively captured in sediments when dissolved sulphide levels in the water column are high (Neubert *et al.*, 2008). Processes that cause sedimentary archives to deviate from capturing dissolved  $\delta^{98}\text{Mo}$  consistently favour the light isotopes (Siebert *et al.*, 2006). Our maximum value of +1.19 ‰ therefore provides a minimum constraint for the composition of dissolved Mo. This result agrees with previous estimates for seawater from mid-Proterozoic basins (+1.0 ‰ to +1.3 ‰, Kendall *et al.*, 2015). We discount a non-marine interpretation because such heavy  $\delta^{98}\text{Mo}$  values are only known from catchments marked by weathering of pyrite- or sulphate-rich rock (Neubert *et al.*, 2011), which was not the case here. Further, although the Stac Fada Member is isotopically heavy (+1.15 ‰), it cannot be a major Mo source to the Poll a'Mhuilt Member because the up-section decline in Cr concentrations (Fig. 1) indicates a steady decrease in the proportion of material reworked from the Stac Fada into the Poll a'Mhuilt. Lighter  $\delta^{98}\text{Mo}$  values in the remainder of the succession likely resulted from either partial Mo remobilisation under oxic conditions (Kowalski *et al.*, 2013) or adsorption of isotopically light  $\text{MoO}_4^{2-}$  onto Fe-oxides (Goldberg *et al.*, 2009).

## Conclusion

The combined geochemical data and sedimentary features characterising the middle Poll a'Mhuilt Member are most parsimoniously interpreted as recording a marine influence on deposition, which calls into question previous inferences that purely non-marine lakes offered particularly favourable conditions for eukaryotic organisms in the Mesoproterozoic (Parnell *et al.*, 2010, 2015). A high bar should be set for arguments favouring non-marine settings in palaeobiological studies because such an assertion carries profound implications for physiological and



biochemical characteristics of early life, as well as for its evolutionary history in marine settings. In the light of our data, the importance of non-marine environments in the expansion of eukaryotic life remains unknown.

## Acknowledgements

Funding for this project was provided by the NASA postdoctoral program (EES), the Lewis and Clark Fund (EES), an NSERC PGS-D grant (EJB), the NSF ELT (TWL, NJP) and FESD (TWL) programs, and the NASA Astrobiology Institute (TWL, NJP). We thank Bleuenn Gueguen, Steve Bates and Andy Robinson for technical assistance.

Editor: Liane G. Benning

## Additional Information

**Supplementary Information** accompanies this letter at [www.geochemicalperspectivesletters.org/article1725](http://www.geochemicalperspectivesletters.org/article1725)

**Reprints and permission information** are available online at <http://www.geochemicalperspectivesletters.org/copyright-and-permissions>

**Cite this letter as:** Stüeken, E.E., Bellefroid, E.J., Prave, A., Asael, D., Planavsky, N.J., Lyons, T.W. (2017) Not so non-marine? Revisiting the Stoer Group and the Mesoproterozoic biosphere. *Geochem. Persp. Let.* 3, 221–229.

## References

- BANNER, J.L., HANSON, G.N. (1990) Calculation of simultaneous isotopic and trace element variations during water-rock interaction with applications to carbonate diagenesis. *Geochimica et Cosmochimica Acta* 54, 3123–3137.
- BARTLEY, J.K., KAH, L.C. (2004) Marine carbon reservoir,  $C_{org}$ - $C_{carb}$  coupling, and the evolution of the Proterozoic carbon cycle. *Geology* 32, 129–132.
- CLOUD, P., GERMS, A. (1971) New pre-paleozoic nannofossils from the Stoer formation (Torridonian), Northwest Scotland. *Geological Society of America Bulletin* 82, 3469–3474.
- DAVIES, N.S., RYSEL, M.C., GIBLING, M.R. (2010) Marine influence in the Upper Ordovician Juniata Formation (Potters Mills, Pennsylvania): implications for the history of life on land. *Palaios* 25, 527–539.
- DAVIS JR., R.A. (2012) Tidal signatures and their preservation potential in stratigraphic sequences. In: Davis Jr., R.A., Dalrymple, R.W. (Eds.) *Principles of Tidal Sedimentology*. Springer, Netherlands, 35–55.
- GOLDBERG, T., ARCHER, C., VANCE, D., POULTON, S.W. (2009) Mo isotope fractionation during adsorption to Fe (oxyhydr) oxides. *Geochimica et Cosmochimica Acta* 73, 6502–6516.
- KAH, L.C., LYONS, T.W., FRANK, T.D. (2004) Low marine sulphate and protracted oxygenation of the Proterozoic biosphere. *Nature* 431, 834–838.

- KENDALL, B., KOMIYA, T., LYONS, T.W., BATES, S.M., GORDON, G.W., ROMANIELLO, S.J., JIANG, G., CREASER, R.A., XIAO, S., MCFADDEN, K., SAWAKI, Y., TAHATA, M., SHU, D., HAN, J., LI, Y., CHU, X., ANBAR, A.D. (2015) Uranium and molybdenum isotope evidence for an episode of widespread ocean oxygenation during the late Ediacaran Period. *Geochimica et Cosmochimica Acta* 156, 173–193.
- KOWALSKI, N., DELLWIG, O., BECK, M., GRÄWE, U., NEUBERT, N., NÄGLER, T.F., BADEWIEN, T.H., BRUMSACK, H.J., VAN BEUSEKOM, J.E., BÖTTCHER, M.E. (2013) Pelagic molybdenum concentration anomalies and the impact of sediment resuspension on the molybdenum budget in two tidal systems of the North Sea. *Geochimica et Cosmochimica Acta* 119, 198–211.
- KUZNETSOV, A.B., SEMIKHATOV, M.A., GOROKHOV, I.M. (2014) The Sr isotope chemostratigraphy as a tool for solving stratigraphic problems of the Upper Proterozoic (Riphean and Vendian). *Stratigraphy and Geological Correlation* 22, 553–575.
- LIU, C., WANG, Z., RAUB, T.D. (2013) Geochemical constraints on the origin of Marinoan cap dolostones from Nuccaleena Formation, South Australia. *Chemical Geology* 351, 95–104.
- LUO, G., ONO, S., HUANG, J., ALGEO, T.J., LI, C., ZHOU, L., ROBINSON, A., LYONS, T.W., XIE, S. (2014) Decline in oceanic sulfate levels during the early Mesoproterozoic. *Precambrian Research*, 258, 36–47.
- LYON, T.D.B., GILLEN, C., BOWES, D.R. (1975) Rb-Sr isotopic studies near the major Precambrian junction, between Scourie and Loch Laxford, northwest Scotland. *Scottish Journal of Geology* 11, 333–337.
- NEUBERT, N., HERI, A.R., VOEGELIN, A.R., NÄGLER, T.F., SCHLUNEGGER, F., VILLA, I.M. (2011) The molybdenum isotopic composition in river water: constraints from small catchments. *Earth and Planetary Science Letters* 304, 180–190.
- NEUBERT, N., NÄGLER, T.F., BÖTTCHER, M.E. (2008) Sulfidity controls molybdenum isotope fractionation into euxinic sediments: Evidence from the modern Black Sea. *Geology* 36, 775–778.
- PARNELL, J., BOYCE, A.J., MARK, D., BOWDEN, S., SPINKS, S. (2010) Early oxygenation of the terrestrial environment during the Mesoproterozoic. *Nature* 468, 290–293.
- PARNELL, J., MARK, D., FALICK, A.E., BOYCE, A., THACKREY, S. (2011) The age of the Mesoproterozoic Stoer Group sedimentary and impact deposits, NW Scotland. *Journal of the Geological Society* 168, 349–358.
- PARNELL, J., SPINKS, S., ANDREWS, S., THAYALAN, W., BOWDEN, S. (2015) High Molybdenum availability for evolution in a Mesoproterozoic lacustrine environment. *Nature Communications* 6, doi:10.1038/ncomms7996.
- POULTON, S.W., CANFIELD, D.E. (2011) Ferruginous conditions: a dominant feature of the ocean through Earth's history. *Elements* 7, 107–112.
- RAISWELL, R., CANFIELD, D.E. (1998) Sources of iron for pyrite formation in marine sediments. *American Journal of Science* 298, 219–245.
- REDDY, S.M., JOHNSON, T.E., FISCHER, S., RICKARD, W.D.A., TAYLOR, R.J.M. (2015) Precambrian reidite discovered in shocked zircon from the Stac Fada impactite, Scotland. *Geology* 43, 899–902.
- REINHARD, C.T., PLANAVSKY, N.J., ROBBINS, L.J., PARTIN, C.A., GILL, B.C., LALONDE, S.V., BEKKER, A., KONHAUSER, K.O., LYONS, T.W. (2013) Proterozoic ocean redox and biogeochemical stasis. *Proceedings of the National Academy of Sciences*, 110, 5357–5362.
- SCOTT, C., LYONS, T.W. (2012) Contrasting molybdenum cycling and isotopic properties in euxinic versus non-euxinic sediments and sedimentary rocks: refining the paleoproxies. *Chemical Geology* 324, 19–27.
- SHIELDS, G., VEIZER, J. (2002) Precambrian marine carbonate isotope database: Version 1.1. *Geochemistry Geophysics Geosystems* 3, doi: 10.1029/2001GC000266.



- SIEBERT, C., MCMANUS, J., BICE, A., POULSON, R., BERELSON, W.M. (2006) Molybdenum isotope signatures in continental margin marine sediments. *Earth and Planetary Science Letters* 241, 723–733.
- SPENCER, J.E., PATCHETT, P.J. (1997) Sr isotope evidence for a lacustrine origin for the upper Miocene to Pliocene Bouse Formation, lower Colorado River trough, and implications for timing of Colorado Plateau uplift. *Geological Society of America Bulletin* 109, 767–778.
- STEWART, A.D. (1988) The Stoer Group, Scotland. In: Winchester, J.A. (Ed.) *Later Proterozoic stratigraphy of the North Atlantic regions*. Blackie, Glasgow, 97–103.
- STEWART, A.D. (2002) *The later Proterozoic Torridonian rocks of Scotland: Their sedimentology, geochemistry and origin*. Geological Society, Bath, UK.
- STEWART, A.D., PARKER, A. (1979) Palaeosalinity and environmental interpretation of red beds from the late Precambrian ('Torridonian') of Scotland. *Sedimentary Geology* 22, 229–241.
- VEIZER, J., CLAYTON, R.N., HINTON, R.W., VON BRUNN, V., MASON, T.R., BUCK, S.G., HOEFS, J. (1990) Geochemistry of Precambrian carbonates: 3-shelf seas and non-marine environments of the Archean. *Geochimica et Cosmochimica Acta* 54, 2717–2729.

